What governs the interannual variability of recurving North Atlantic tropical cyclones?

Sainsbury, E. M., Schiemann, R. K. H. ORCID: https://orcid.org/0000-0003-3095-9856, Hodges, K. I., Baker, A. J. ORCID: https://orcid.org/0000-0003-2697-1350, Shaffrey, L. C. ORCID: https://orcid.org/0000-0003-2696-752X and Bhatia, K. T. (2022) What governs the interannual variability of recurving North Atlantic tropical cyclones? Journal of Climate, 35 (12). pp. 3627-3641. ISSN 1520-0442 doi: https://doi.org/10.1175/JCLI-D-21-0712.1 Available at https://centaur.reading.ac.uk/103982/

What Governs the Interannual Variability of Recurving North Atlantic Tropical Cyclones?

ELLIOTT M. SAINSBURY,[a] REINHARD K. H. SCHIEMANN,[b] KEVIN I. HODGES,[b] ALEXANDER J. BAKER,[b] LEN C. SHAFFREY,[b] AND KIERAN T. BHATIA[c]

[a] *Department of Meteorology, University of Reading, Reading, Berkshire, United Kingdom*
[b] *National Centre for Atmospheric Science, University of Reading, Reading, Berkshire, United Kingdom*
[c] *Guy Carpenter, New York, New York*

(Manuscript received 8 September 2021, in final form 14 February 2022)

ABSTRACT: Recurving tropical cyclones (TCs) can cause extensive damage along the U.S. East Coast and later in their life cycle over Europe as post-tropical cyclones. While the existing literature attempts to understand the drivers of basin-wide and regional TC variability, less work has been undertaken looking at recurving TCs. The roles played by the interannual variabilities of TC frequency and the steering flow in governing recurving TC interannual variability are investigated in this study. Using a track-matching algorithm, we identify observed TC tracks from the NHC "best track" hurricane database, version 2 (HURDAT2) in the ERA5 and MERRA2 reanalyses. This allows for detailed analysis of the post-tropical stages of the tracks in the observational TC record, enabling robust identification and separation of TCs that recurve. We show that over 75% of the interannual variance in annual recurving TC frequency can be explained by just two predictors—the frequency of TCs forming in the subtropical Atlantic, and hurricanes (TCs with wind speeds > 33 m s^{-1}) forming in the main development region (MDR). An index describing the seasonal mean meridional steering flow shows a weak, nonsignificant relationship with recurving TC frequency, supported by composite analysis. These results show that the interannual variability in recurving TC frequency is primarily driven by the seasonal TC activity of the MDR and the subtropical Atlantic, with seasonal anomalies in the steering flow playing a much smaller, secondary role. These results help to quantify the extent to which skillful seasonal forecasts of Atlantic hurricane activity benefit regions vulnerable to recurving TCs.

SIGNIFICANCE STATEMENT: Recurving tropical cyclones (TCs) can cause extensive damage to the U.S. East Coast, eastern Canada, and Europe. It is, therefore, crucial to understand why some years have a higher frequency of recurving TCs than other years. In this study, we show that the frequency of recurving TCs is very strongly linked to the frequency that hurricanes (TCs with wind speeds > 33 m s^{-1}) form in the main development region, and the frequency that TCs form in the subtropical Atlantic. This result suggests that skillful seasonal prediction of hurricane activity could be used to give enhanced seasonal warning to the regions often impacted by recurving TCs.

KEYWORDS: Extratropical transition; Hurricanes/typhoons; Tropical cyclones; Interannual variability

1. Introduction

Recurving North Atlantic tropical cyclones (TCs) can pose extreme hazards to the U.S. East Coast, and later in their life cycle over Europe. For example, Hurricane Sandy led to over 200 deaths, many of which were in the northeastern United States, a region that does not often see direct impacts from TCs. At the time, Sandy was the second costliest TC in U.S. history, causing over $65 billion USD in damages (Blake et al. 2013).

The steering flow played a clear role in the unusual track of Hurricane Sandy. A ridge over the northwest Atlantic Ocean drove a southeasterly steering flow toward the Northeast United States. The steering effect of the ridge, along with favorable interaction with an upper-level trough to the northwest, were ultimately responsible for the strength and track of Sandy in the latter stages of its life cycle (Varlas et al. 2019). For a TC to be classified as recurving using existing methods (such as described in Archambault et al. 2013; Riboldi et al. 2018), a TC must change its direction of travel from westward to eastward while traveling poleward. TCs like Sandy that traveled northwest and then northeast for a time would therefore be classified as recurving TCs, even though they might not traditionally be thought of as recurving TCs (as they do not have the classical "C" shape track). In this study, we are interested in TCs that pose risk to land regions in the North

Denotes content that is immediately available upon publication as open access.

Supplemental information related to this paper is available at the Journals Online website: https://doi.org/10.1175/JCLI-D-21-0712.s1.

Corresponding author: Elliott M. Sainsbury, e.sainsbury@pgr.reading.ac.uk

DOI: 10.1175/JCLI-D-21-0712.1

Atlantic midlatitudes (such as the U.S. East Coast and Europe). We therefore define a recurving TC as any North Atlantic TC that enters the North Atlantic midlatitudes in the domain 36°–70°N, 82°W–30°E with no requirement for a change in zonal direction of travel.

Recurving TCs can also cause damage across Europe (Dekker et al. 2018; Laurila et al. 2020), particularly in the form of extreme precipitation, strong winds and large waves (Evans et al. 2017; Jones et al. 2003). Ex-Hurricane Ophelia was responsible for Ireland's strongest wind gust on record of 119 mph in 2017, and ex-Hurricane Charley brought severe flooding to parts of the United Kingdom and Ireland in 1986 (Hickney and Connolly-Johnston 2012). Post-tropical cyclones (PTCs) are a robust feature of midlatitude and European storminess during hurricane season (Baker et al. 2021) but are also disproportionately responsible for high impact windstorm risk. Recent work has shown that, despite accounting for less than 1% of all cyclones to impact northern Europe during the North Atlantic hurricane season, PTCs represent 9% of all cyclones with storm-force (>25 m s^{-1}) winds (Sainsbury et al. 2020).

Given the risk associated with recurving TCs to the U.S. East Coast and later in their life cycle over Europe, it is crucial to understand what governs the interannual variability of the frequency of recurving TCs. One possible driver of recurving TC frequency is basinwide TC frequency. The 2005 North Atlantic hurricane season produced 16 recurving TCs, more than any other year considered in this study (1979–2018). This year also contained the highest number of TCs in the North Atlantic. The greater the number of TCs in the North Atlantic, then the more opportunities there are for TCs to recurve. It is therefore hypothesized that TC frequency is strongly associated with recurving TC frequency.

The physical drivers of basinwide TC frequency are well understood, with contemporary statistical, dynamical (e.g., Camp et al. 2015; Murakami et al. 2016b,) and hybrid models now exhibiting good skill at predicting basinwide TC activity before the onset of peak hurricane season activity (Klotzbach et al. 2019). Forecasts and observations of large-scale environmental fields over the tropical North Atlantic during and prior to hurricane season, which have been shown to have a strong physical link with hurricane season activity (Saunders et al. 2017) explain approximately 60% of the variance in hurricane season activity, allowing for skillful seasonal forecasts from 1 July (Klotzbach 2014).

Boudreault et al. (2017), Kossin et al. (2010) and Kozar et al. (2012) use various clustering techniques to segregate North Atlantic TCs into four different groups, in order to understand the drivers of the interannual variability in these groups of TCs. It was found that the frequency with which TCs form in the deep tropics is strongly modulated by the Atlantic meridional mode (AMM) and El Niño–Southern Oscillation (ENSO), whereas higher latitude TC frequency is modulated by the NAO (Elsner et al. 2000; Kossin et al. 2010). The frequency with which storms form in the Gulf of Mexico is also strongly modulated by ENSO (Boudreault et al. 2017), whereas the frequency with which storms originate in the northern and eastern parts of the basin are modulated by the subtropical high (Kozar et al. 2012).

While the steering flow on the daily time scale is important for the evolution and track of recurving TCs (such as in the case of Sandy), the role of the steering flow on the seasonal time scale is not as well understood. However, as the mean steering flow may alter the typical trajectory of TC tracks over the hurricane season, it may modulate recurving TC frequency. The seasonal mean steering flow is therefore a second possible driver of recurving TC frequency.

By subsampling the HURDAT database to investigate main development region (MDR) storms only, Colbert and Soden (2012) investigate the role of the steering flow on North Atlantic hurricane tracks by segregating storms into three categories based on recurvature: straight moving, recurving land and recurving ocean. It was found that recurving ocean storms were associated with a weakening of the North Atlantic subtropical high (NASH) on the time scale of individual storms. On the seasonal time scale, the fraction of storms that ended up in the recurving ocean category was highest during El Niño years and years with a positive AMM. Recent work has also shown that during strong Indian monsoon years, the strength of the NASH is enhanced, leading to increased landfall probability of MDR TCs (Kelly et al. 2018).

The relative importance of the interannual variabilities in hurricane season activity (TC frequency) and steering flow in the North Atlantic to recurving TCs remains unknown from a climate perspective. In this paper, we investigate the relative importance of both the interannual variabilities of the seasonal mean steering flow and TC frequency in governing recurving TC frequency in the North Atlantic. This is achieved by constructing a statistical model to quantify the variance in recurving TC frequency that can be explained by regional TC activity, and by presenting a composite analysis to investigate the role of the steering flow on the seasonal time scale.

The paper continues in section 2 with a description of the data used, along with details of the TC feature-tracking scheme, the spectral filtering technique used to isolate the background flow, and an objective track-matching algorithm used to identify recurvature. Section 3 contains an analysis of track and genesis differences between recurving and nonrecurving TCs, a composite analysis to investigate the role of the steering flow, and an analysis of the statistical model. The paper concludes with a summary and discussion in section 4.

2. Methods and data

Observational best track data do not always contain information on the position and intensity of TCs after they have been designated as post-tropical (Hagen et al. 2012; Delgado et al. 2018). In addition, the eastern boundary of the National Hurricane Center (NHC) area of responsibility was only extended eastward from 35°W to the coasts of Africa and western Europe in 2005 (Rappaport et al. 2009), possibly introducing more inhomogeneities to the observational record for TC tracks. TC tracks are often limited to their tropical phase, making it difficult to consistently separate the TCs that

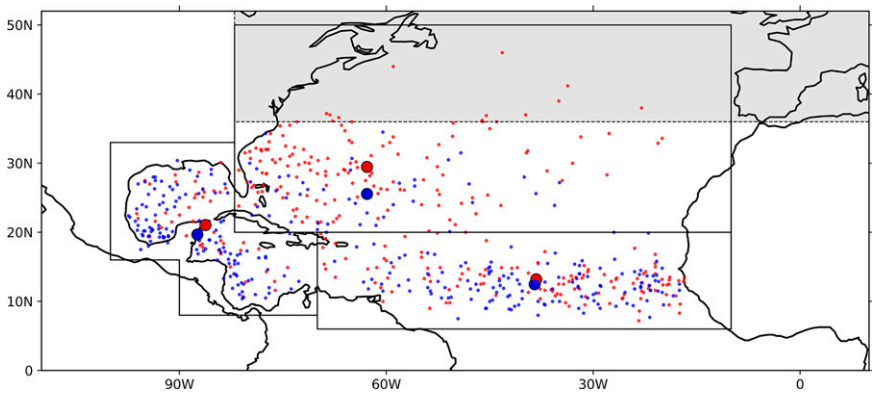

FIG. 1. Genesis location (HURDAT2) of all recurving (red) and non-recurving (blue) TCs forming in the North Atlantic from 1979 to 2018. The three domains overlaid represent the three sampling regions used in this study: MDR (lower right), SUB (upper right), and WEST (left). The shaded region represents the domain used to define recurvature. Larger dots represent the mean genesis location in HURDAT2 for the tracks in the region.

recurve from those that do not when using best track data. To overcome this, we first track all Northern Hemisphere cyclonic features in two reanalysis datasets. We then use an objective track matching method to identify the TCs in the NHC "best track" hurricane database, version 2 (HURDAT2; Landsea and Franklin 2013), which are present in these reanalyses, thereby giving us an extended track that includes the storms' post-tropical evolution. A TC is then classified as either recurving or non-recurving depending on whether the corresponding track in the reanalysis enters a domain in the North Atlantic from 36°–70°N to 82°W–30°E. A boundary of 36°N was chosen because almost all (~98%) TC genesis in the North Atlantic occurs equatorward of this latitude band (see Fig. 1), so for a TC to enter this domain it (almost always) gains latitude. A western boundary of 82°W is used because this allows for all TCs traversing the East Coast to be identified as recurving, along with those that recurve farther east in the basin. The sensitivity of the results presented here have been tested on a second domain, extending from 36°–70°N to 70°W–30°E, to ensure that results are robust to changes in the definition of recurvature.

a. Datasets

Two different reanalyses are used to test the sensitivity of our results to the reanalysis product. We use the ERA5 (Hersbach et al. 2020) and MERRA2 (Molod et al. 2015; Gelaro et al. 2017) reanalyses to provide the 6-hourly relative vorticity fields that are necessary for the cyclone detection and tracking scheme (600, 700, and 850 hPa, vertically averaged). We also use 6-hourly wind (u and v) fields at 200-, 500-, 700-, and 850-hPa pressure levels to construct seasonal mean wind fields for composite analysis and for the construction of a meridional steering flow index. The 6-hourly mean sea level pressure (MSLP) data are also used after removing the TC vortices to construct seasonal means for composite analysis.

ERA5 is based on the Integrated Forecasting System cycle 41r2. Data from 1979 to 2018 are used because despite being available, the back-extension to 1950 is not yet deemed suitable by the ECMWF for TC analysis due to an unrealistic representation of TC intensity (Bell et al. 2021). ERA5 is chosen based on its high horizontal resolution and four-dimensional variational data assimilation scheme, which have been shown in previous reanalyses to improve the representation of the location and intensity of TCs. MERRA2 uses the GEOS 5.12.4 data assimilation system, which comprises the GEOS atmospheric model and GSI analysis scheme (Gelaro et al. 2017). MERRA2 data are used from 1980 to 2016. The figures presented in this paper contain ERA5 data only, and corresponding figures created using MERRA2 data are available in the supplemental material (Figs. S1–S4, S10). This is done for simplicity and to avoid duplication, because the MERRA2 results in the supplement are very similar to the results presented in the main manuscript. Observational best track data from the HURDAT2 are also used between 1979 and 2018.

b. Spectral filtering

Spectral filtering using a spectral transform based on spherical harmonics is utilized in two different ways in this study, using the functionality of the cyclone detection and tracking scheme, TRACK (section 2c). In the first instance, spectral filtering is applied to the relative vorticity fields necessary to detect and track the cyclones. The vertically averaged 600–850-hPa relative vorticity field is spectrally filtered to a spectral resolution of T63 (approximately equivalent to 200 km in the midlatitudes), and waves with a total wavenumber of less than 6 are removed. This removes the smallest horizontal scales and the planetary scale waves, isolating the vorticity scales relevant for cyclone detection and tracking.

Section 3c contains composite analysis that is used to investigate the large-scale environmental flow during years of high and low recurving TC activity. To ensure that the fields used contain a minimal signature of the recurving TC vortices themselves, the reanalysis data are also spectrally filtered. This is performed on the global, 6-hourly reanalysis fields for MSLP and wind (u and v). The data are truncated to a T11

spectral resolution (approximately 10° × 10°) globally (but output on the original grid), which removes approximately 95% of the circulation associated with the vortices. For further information, see Bhatia et al. (2020). On the seasonal time scale used in this paper the differences between the spectrally filtered flow and the nonfiltered flow are relatively small. Some differences exist in the composite plots (Figs. 4–6) depending on whether spectrally filtered data are used or not (see Fig. S9 in the online supplemental material). However, these differences do not alter the interpretation of the figures. For consistency, the spectrally filtered data are used throughout.

c. Cyclone detection and tracking

Cyclone detection and tracking is performed using the tracking scheme of Hodges (1994, 1995, 1999) (named TRACK) configured for TCs. Vertically averaged 6-hourly relative vorticity fields at the 600-, 700-, and 850-hPa pressure levels are used to perform the tracking. The vertically averaged vorticity is first spectrally filtered as described in section 2b. Features are first identified with a T63 vorticity maximum exceeding 0.5×10^{-5} s^{-1}, and then refined by identifying the off-grid locations using B-spline interpolation and maximum ascent optimization (Hodges 1994). These features are tracked and retained as cyclones. Tracks that have a lifetime less than two days are then removed. Further details on the configuration of the tracking scheme used in this study are available in Hodges et al. (2017). Cyclone detection and tracking is performed for the entire Northern Hemisphere for both reanalyses, and systems that pass though the North Atlantic basin are then selected.

d. Objective track matching

A reanalysis cyclone track matches that of a HURDAT2 track if there is temporal overlap of the 6-hourly time steps and the mean separation distance between the reanalysis track and the HURDAT2 track is less than 4 geodesic degrees for all overlapping time steps. If there is more than one reanalysis cyclone track that satisfies this criterion, then the reanalysis cyclone track that has the smallest mean separation distance to the HURDAT2 track is chosen (Hodges et al. 2017; Hodges and Emerton 2015). A small proportion (~5%) of the TCs in HURDAT2 are not identified in the ERA5 and MERRA2 reanalyses and are excluded from the analysis. These tend to be weak, short-lived systems (Sainsbury et al. 2020) and their exclusion does not affect the results of this study.

e. Track and genesis density statistics

The spherical kernel method of Hodges (1996) is used to show the spatial distribution of the TC tracks. Statistical significance in the spatial distribution differences of recurving and non-recurving TCs is tested using the Monte Carlo approach described in Hodges (2008). Densities are calculated per unit area per year, where the unit area is equivalent to a spherical cap with a radius of 5°.

f. Regional selection and recurvature definition

The matched TCs are separated according to three regions (shown in Fig. 1), based on their genesis location in HURDAT2. These three regions are the MDR (10°–70°W, 6°–20°N), subtropical Atlantic (SUB, 10°–82°W, 20°–50°N), and the region comprising the Gulf of Mexico and south Caribbean, denoted WEST [(8°N, 70°W), (8°N, 90°W), (16°N, 90°W), (16°N, 100°W), (33°N, 100°W), (33°N, 82°W), (20°N, 82°W), and (20°N, 70°W)]. The choice of three regions is subjective, but the regions themselves each have a physical basis. The MDR TCs typically form from African easterly waves unlike the TCs in the other two regions (Caron and Jones 2012; Arnault and Roux 2011). In the SUB region, TCs often form under marginal conditions for tropical cyclogenesis. This region also contains TCs that form via tropical transition, with precursors of extratropical origin (Kossin et al. 2010). The TCs forming in region WEST often encounter the most favorable thermodynamic conditions for intensification [e.g., see potential intensity map (Fig. 3) in Camargo et al. (2013)], with the main inhibitor of intensification often being the proximity to land. The three regions also have broadly different seasonal mean values of vertical wind shear (e.g., Fig. 3 in Aiyyer and Thorncroft 2006). The three chosen regions therefore allow for a zonal and meridional separation of tracks based on genesis, thermodynamic and dynamic conditions, and precursor type.

The choice is made to group storms into these three regions based on the factors that may be important for recurvature. An obvious factor is proximity to the midlatitudes—a TC forming at higher latitudes is unlikely to be influenced by the strongest easterly trades that steer TCs zonally, and thus may be more likely to recurve. A second justification is the differing thermodynamical and dynamical conditions in the three regions, which largely control the lifetime maximum intensity (LMI) of the TCs. TCs that form in regions climatologically more conducive for intensification will often attain higher intensities, and the resilience associated with stronger TCs is likely key to their longevity and ability to maintain their structure in hostile environments, which may lead to an increased probability of recurvature.

Many studies (e.g., Boudreault et al. 2017; Kossin et al. 2010; Kozar et al. 2012) use clustering methods to group TCs, rather than regional boundaries that are used here and in Colbert and Soden (2012). Despite these differences in methodology, the three TC regions used here can be related to the TC classifications used in other studies. TCs in SUB, WEST, and MDR are closely related to clusters 1, 2, and 3, respectively, in Kossin et al. (2010) and Kozar et al. (2012). Cluster 4 in these studies mainly relates to TCs forming in the MDR and WEST regions. TCs forming in the SUB and WEST regions are similar to clusters 1 and 2 in Boudreault et al. (2017), with clusters 3 and 4 in this study relating to MDR recurving and MDR non-recurving TCs, respectively. These three previous studies all used a similar clustering technique, which is more readily able to distinguish tracks based on their genesis location than the *K*-means method used in many other studies of TC clustering (e.g., Harr and Elsberry 1995).

The TCs in each region are designated as recurving if their ERA5/MERRA2 matched track enters the domain defined as 36°–70°N, 82°W–30°E (shaded box, Fig. 1). This method for identifying recurvature is different to that used by Colbert and Soden (2012), in which the degree of recurvature (either straight-moving, recurving-land, or recurving-ocean) associated with a TC is determined based on which spatial boundary the HURDAT TC track intersects. Our method of vorticity-based tracking allows us to extrapolate the TC tracks present in HURDAT2, giving us a more robust separation of tracks based on their recurvature.

g. *Multiple linear regression model*

We use multiple linear regression to quantify the variability in recurving TC frequency that is associated with TC activity in the North Atlantic. There are several candidates for predictors, including basinwide TC frequency and regional TC frequency in the North Atlantic, with and without intensity constraints. Using the analysis presented in sections 3a and 3b, a multiple linear regression model is fit using the two most suitable predictors:

$$\mathrm{Rec_{TC}} = \beta_0 + \beta_1 x_1 + \beta_2 x_2 + \epsilon, \quad (1)$$

where β_0, β_1, and β_2 are coefficients to be fitted, x_1, x_2 are the two chosen predictors, and ϵ represents the residuals.

3. Results

a. *Historical TC recurvature statistics*

Figure 1 shows the genesis location for all TCs in HURDAT2 between 1979 and 2018, along with the boundaries for each of the three regions that the TCs are separated into. The shaded region represents the domain used to define recurvature. It should be noted that there is an overlap between the SUB region and the recurvature domain, with 12 TCs (<2% of all TCs considered in this study) identified as recurving by virtue of their genesis location. The sensitivity of the results to these overlapping TCs has been tested, and the results remain unchanged whether they are excluded from the analysis or not. As a result, we include these TCs in the analysis of this paper. The SUB region is the largest spatially and contains the largest number of recurving TCs of any of the three regions. It also contains the highest fraction of recurving TCs at 76.6% (Table 1). TCs forming in this region form poleward of the strongest easterly trade winds and are also closer to the midlatitude westerly flow. The mean genesis latitude of recurving SUB TCs is 4° farther poleward than for the non-recurving TCs (29.5° and 25.5°N for recurving and non-recurving TCs, respectively), and this difference is significant to 95% using a Student's *t* test.

The MDR contains the largest number of TCs of any of the three regions, approximately 48% of which recurve. The mean longitude of genesis for TCs in this region is similar for both recurving and non-recurving TCs at 38.3° and 38.5°W, respectively. Although small, the differences in the mean genesis latitude of recurving and non-recurving TCs in the MDR (13.2° and 12.5°N) are also statistically significant to 95%.

TABLE 1. Summary of the number of recurving, non-recurving, and total TCs, along with the percent of TCs that recurve in each of the three sampling regions displayed in Fig. 1. The right-hand column gives the basinwide statistics.

	MDR	SUB	WEST	Whole North Atlantic
Recurving	121	144	48	313
Non-recurving	130	44	122	296
Total	251	188	170	609
Percent recurving	48.2%	76.6%	28.2%	51.4%

Only a quarter of TCs forming in the WEST region recurve, and TCs in the WEST region account for only 15% of the overall number of recurving TCs. No significant differences in mean position exist between the recurving and non-recurving TCs in this region. Overall, Fig. 1 suggests that both the zonal and meridional location of TC genesis are associated with TC recurvature, with TCs forming in regions farther poleward and eastward in the basin comprising the highest proportion of recurving storms. A summary of this information can be found in Table 1.

b. *Regional historical TC statistics*

1) HISTORICAL TC TRACK AND PRECURSOR GENESIS DENSITIES

Track and genesis densities are calculated for recurving and non-recurving TCs using the ERA5 reanalysis tracks that have been separated by their region of formation as defined by HURDAT2. Genesis densities outside of each region (which are denoted by the red boxes) are nonzero in some areas. This is because we are assigning storms to a region using HURDAT2 genesis location but calculating genesis and track density using the corresponding ERA5 tracks, where the pre-TC life cycle stages are identified. Figure 2 is therefore showing the TC precursor genesis density. Another reason for the nonzero densities outside of the regions is because the densities are calculated for a unit area using the kernel method, with kernels that spread the influence of a data point depending on their bandwidth. Differencing (recurving minus non-recurving) the track and genesis densities will highlight if there are important differences in genesis within regions and will also indicate where in the TCs life cycle the trajectories start to differ. In the MDR and SUB regions, the differences in the track density are meridional—with significant negative (lower recurving TC density) differences equatorward, and positive differences (higher recurving track density) poleward. However, in the WEST region the differences are much more zonal, with more recurving TCs in the east of this region (Fig. 3).

Most of the recurving TCs forming in the MDR cross the northern boundary of the region, whereas the non-recurving MDR TCs mainly track out of the western edge (Figs. 3a,d). Track density values for the non-recurving TCs decrease substantially to the west and north of the MDR region, in part due to a broadening of the distribution from east to west, but also because approximately 40% of the non-recurving MDR

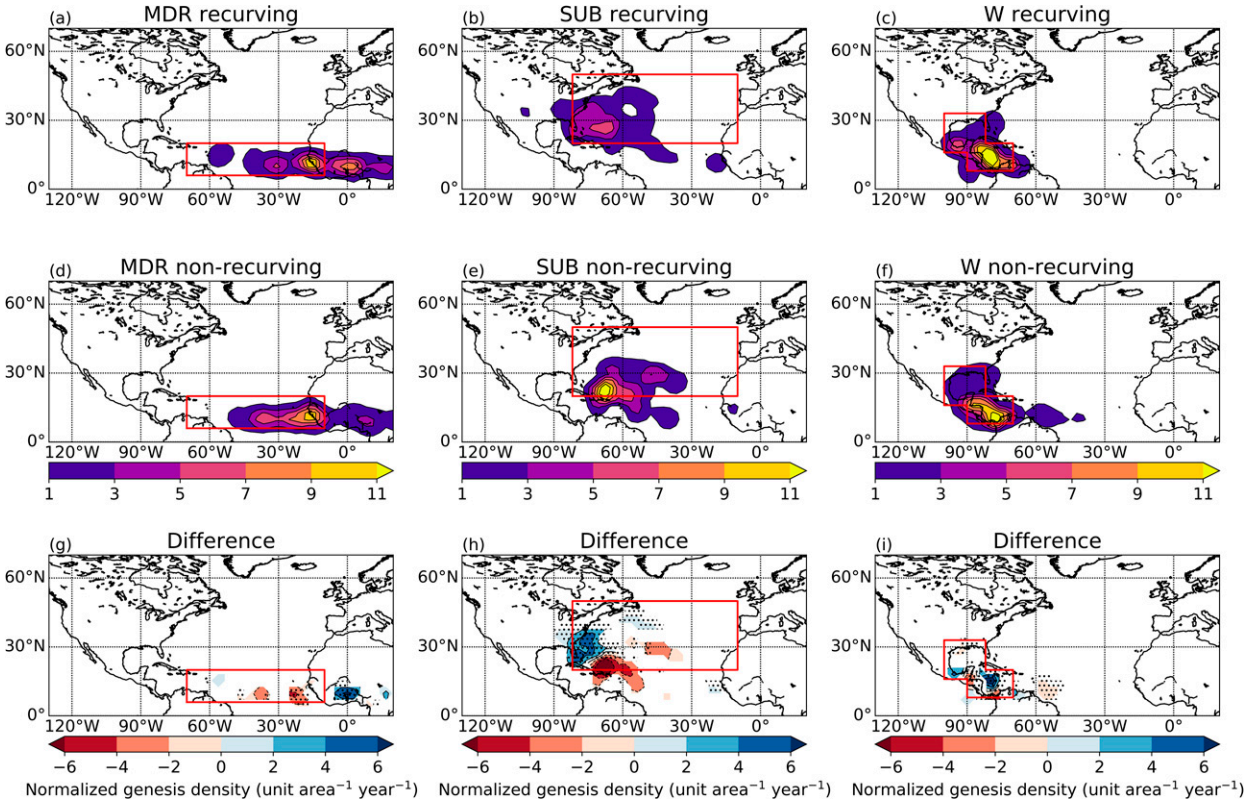

FIG. 2. Normalized genesis density for the (a)–(c) recurving TCs, (d)–(f) non-recurving TCs, and (g)–(i) recurving minus non-recurving in the three sampling regions displayed in Fig. 1. Boundaries for each region are displayed in red. Densities (and differences) less than 1 have been masked for clarity. Stippling denotes significance at the 95% level. Densities are calculated as the number of cyclones per year per unit area, where the area is a 5° radius spherical cap. The densities are normalized to account for differences in sample sizes in (a)–(f) by dividing by the number of cyclones in the sample.

TCs dissipate before leaving the region. Despite these differences in track density, the difference in precursor genesis density in this region is small (Fig. 2g).

Significant differences can be seen in the track and genesis densities for TCs forming in the SUB region, with recurving TCs forming farther north and west than non-recurving TCs, which form primarily on the border between the MDR and SUB regions (Figs. 2b,e). This agrees with the significant difference in the genesis latitude of recurving and non-recurving TCs seen in Fig. 1 and indicates that the location of precursor genesis is also significantly different for the recurving and non-recurving TCs in the SUB region. The non-recurving TCs in the SUB region gain little latitude and either travel eastward and decay in the subtropical North Atlantic or reach the Caribbean and Southeast United States (Fig. 3e).

Few differences exist between the recurving and non-recurving TC genesis densities in the WEST region, but track density differences are seen. The recurving TCs forming in WEST impact the states bordering the eastern side of the Gulf of Mexico, whereas the non-recurving TCs forming in this region often impact Central America. This can be seen in the differenced track density plots for this region (Fig. 3i).

2) LIFETIME MAXIMUM INTENSITY DISTRIBUTIONS

Inherent to TC recurvature is longevity (particularly for storms forming in the MDR)—stronger TCs may be more resilient to hostile environments, and as a result, last longer. For a MDR TC to recurve, it often must endure less than ideal sea surface temperatures, an environment that may be too hostile for most weak TCs. We therefore investigate the lifetime-maximum intensity (LMI) distributions for recurving and non-recurving TCs in the three genesis regions used to partition the TCs. These are shown in Fig. 4. Across much of the North Atlantic basin (WEST and SUB regions), there are small (but statistically significant at 95% by a Kolmogorov–Smirnov test) differences between the LMI distributions of recurving and non-recurving TCs. However, in the MDR there is a large significant difference (Fig. 4a). The non-recurving TCs tend to be considerably weaker at their LMI than recurving TCs. 40% of non-recurving TCs that form in the MDR dissipate before leaving the region, attaining a low LMI.

Recurvature of TCs in the MDR is linked to the strength and westward extent of the North Atlantic subtropical high (NASH) (i.e., the steering flow), with TCs often recurving around the western edge of the high (Colbert and Soden

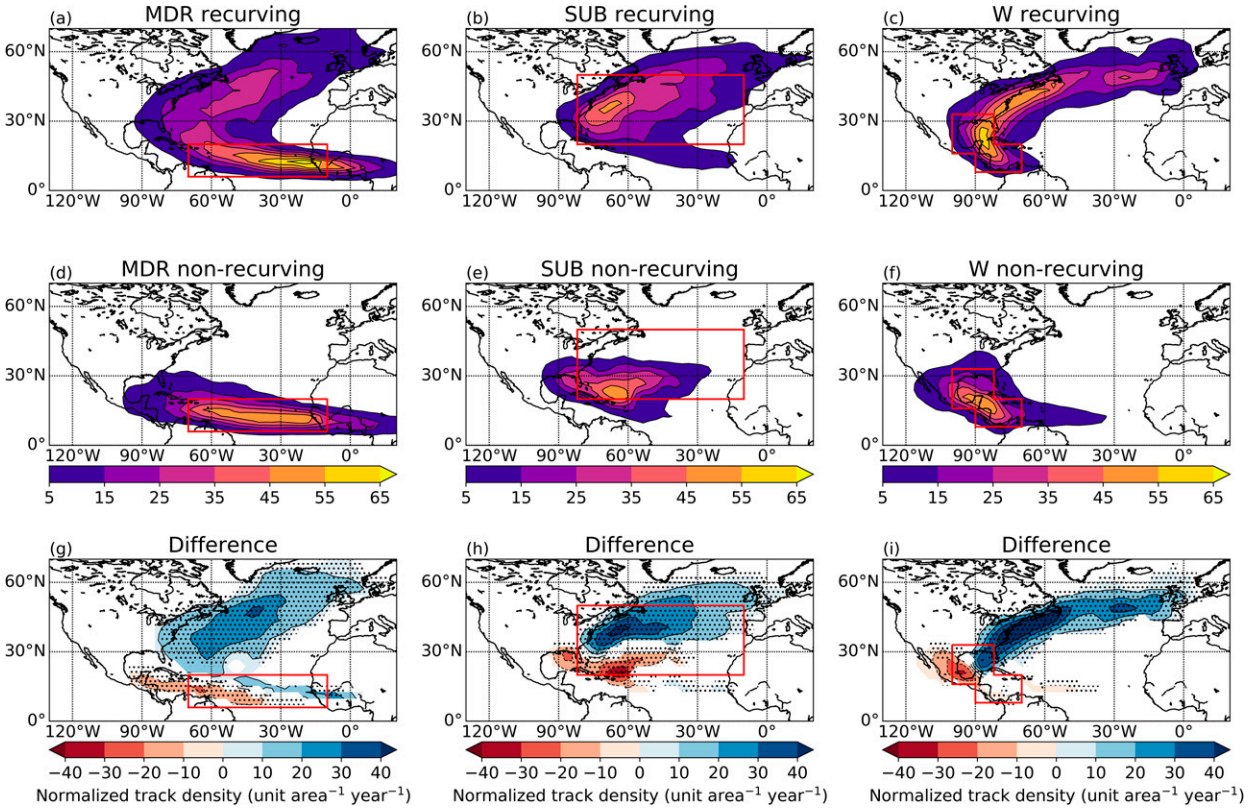

FIG. 3. Normalized track density for the (a)–(c) recurving TCs, (d)–(f) non-recurving TCs, and (g)–(i) recurving − non-recurving TCs in the three sampling regions displayed in Fig. 1. Boundaries for each region are displayed in red. Densities (and differences) less than 5 have been masked for clarity. Stippling denotes significance at the 95% level. Densities are calculated as the number of cyclones per year per unit area, where the area is a 5° radius spherical cap. The densities are normalized to account for differences in sample sizes in (a)–(f) by dividing by the number of cyclones in the sample.

2012). Some MDR TCs die out before reaching the western edge of the subtropical high and as a result, are classified as non-recurving. Another possible reason that recurving TCs have higher LMI is beta drift (Wang et al. 1998). This drift is usually of the order of a few meters per second (Wang et al. 1997) with stronger TCs drifting poleward out of the easterly trade winds faster than weaker TCs (Colbert and Soden 2012). The recurving TCs also have a longer track over the ocean, potentially allowing those tracking over the warm Gulf Stream to attain greater intensities.

c. *Predictors of recurving TC frequency*

In this section, we first explore the role of the steering flow in modulating the number of recurving TCs. In section 3c(1) the focus is on TCs forming in the MDR, and in section 3c(2) we investigate TCs forming in the SUB region.

1) THE STEERING FLOW (MDR)

To investigate the role of the seasonal mean steering flow on TC recurvature for storms originating in the MDR, we use the deep-layer flow, $\mathbf{V}_{\mathrm{DLS}}$ [Eq. (2)], defined previously by Colbert and Soden (2012). The subscripts represent the pressure level (in hPa) at which the flow is used. The MSLP is also used to determine the strength and position of the NASH, the westward extent of which was shown by Colbert and Soden (2012) to modulate TC recurvature from the MDR. In the construction of Figs. 5 and 6, spectral filtering is performed on the MSLP and wind field data as described in section 2b:

$$\mathbf{V}_{\mathrm{DLS}} = 0.25\mathbf{V}_{200} + 0.5\mathbf{V}_{500} + 0.25\mathbf{V}_{850}. \qquad (2)$$

Figures 5a and 6a show the difference in the composite mean August, September, and October (ASO) deep layer flow and MSLP, respectively, between years that have a very high number and a very low number of recurving TCs originating in the MDR, defined as (number > mean + 1 standard deviation) and (number < mean − 1 standard deviation). Figures 5b and 6b show the differences between years that have a high (number > mean) and low (number < mean) number of recurving TCs originating in the MDR. Of the 40 years used in our analysis, 9 years have very high activity, 11 years have very low activity, 17 years have high activity and 23 years have low activity.

Figure 5a shows anomalously strong southeasterlies over the central Subtropical Atlantic during years where there is a very high number of recurving TCs originating in the MDR. Figure 5b also shows the same anomalous meridional flow in

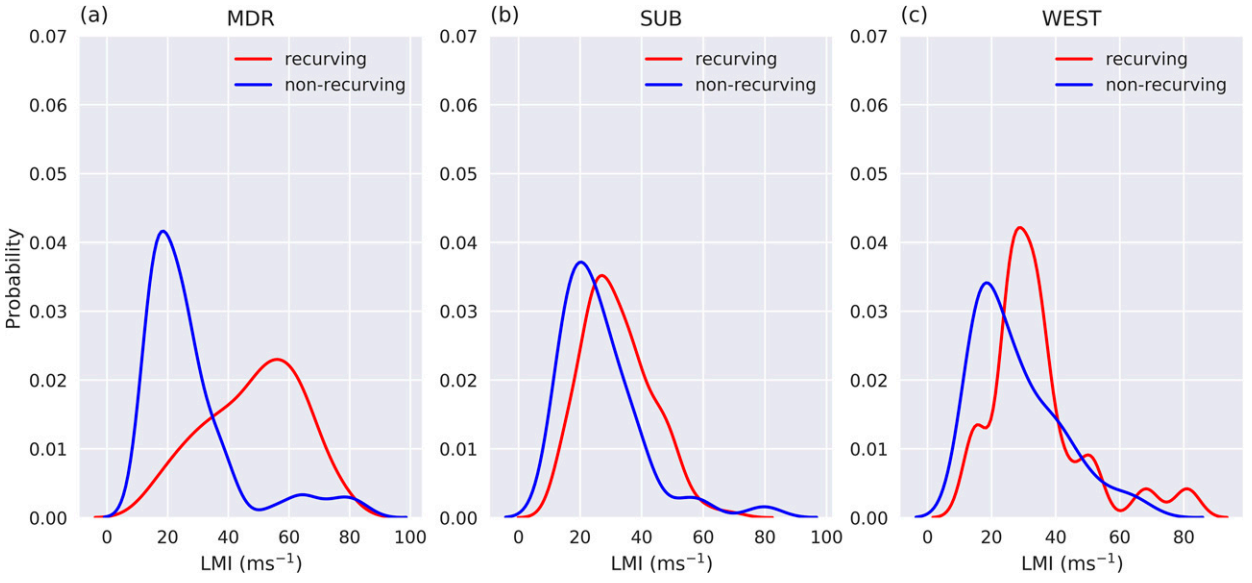

FIG. 4. Probability distributions of Lifetime maximum intensity (LMI) for all recurving (red) and non-recurving (blue) TCs in the North Atlantic, 1979–2018, for the three regions displayed in Fig. 1. Densities have been calculated using a kernel density estimation.

the subtropical Atlantic, but this time centered approximately 10° farther west. This anomalous flow may steer TCs that formed in the MDR on a poleward trajectory, directing them away from the easterly trade winds before they have tracked to the western side of the basin. This is consistent with Fig. 3a, in which the recurving TCs originating in the MDR see an increase in their poleward translation speed in the central Atlantic. At this point in their life cycle, some of the TCs may still be weak. Red contours in Figs. 5a and 5b show the 1550-m 850-hPa geopotential height contour for the composites, to illustrate the westward extent of the NASH. During years of high MDR-originating recurving TC frequency, the westward extent of the NASH is reduced (solid lines) compared to years of low frequency (dashed), in agreement with Colbert and Soden (2012).

The sensitivity of the measure used to characterize the steering flow is tested by replicating the composites using a lower level flow (such as described in Chan and Gray 1982). Recreating Fig. 5 using the 700-hPa flow shows the same anomalous flow pattern as seen in the subtropical Atlantic in Fig. 5; however, in this case the anomalous poleward flow extends farther equatorward in to the MDR (see Fig. S7, supplemental material).

Both Figs. 6a and 6b show a significant negative difference in the ASO MSLP field in the tropical Atlantic and the western subtropical North Atlantic toward the east of the Southeast United States. This suggests that during years when there are a larger number of recurving TCs originating in the MDR, the MSLP in the western subtropical Atlantic is anomalously low. This is physically consistent with the results of Colbert and Soden (2012) and Fig. 5 and is indicative of higher TC recurvature coinciding with reduced westward extent of the NASH. The anomalously low MSLP in the

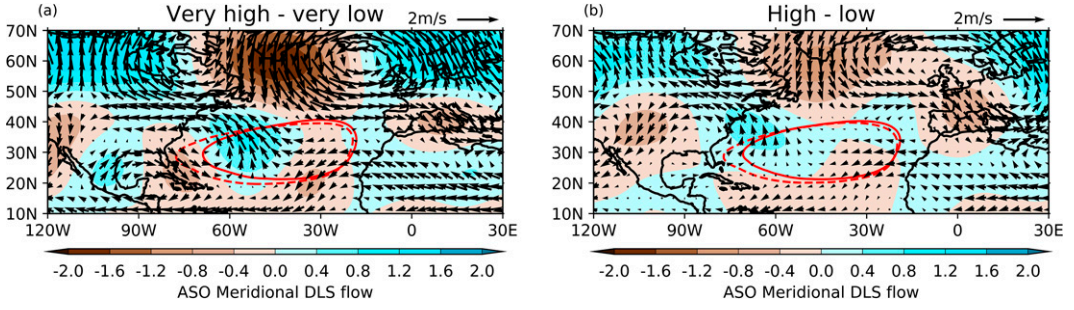

FIG. 5. Composite differences in the deep layer flow (wind vectors), calculated from T11 spectrally filtered wind fields, based on the number of recurving TCs which form in the MDR: (a) very high minus very low and (b) high minus low. Red lines represent the 1550-m contour for the ASO 850-hPa geopotential height during years of very high (solid) and very low (dashed) recurving TC frequency originating in the MDR in (a) and during years of high (solid) and low (dashed) recurving TC frequency originating in the MDR in (b). Filled contours show the composite difference in the meridional component of the ASO deep layer steering flow.

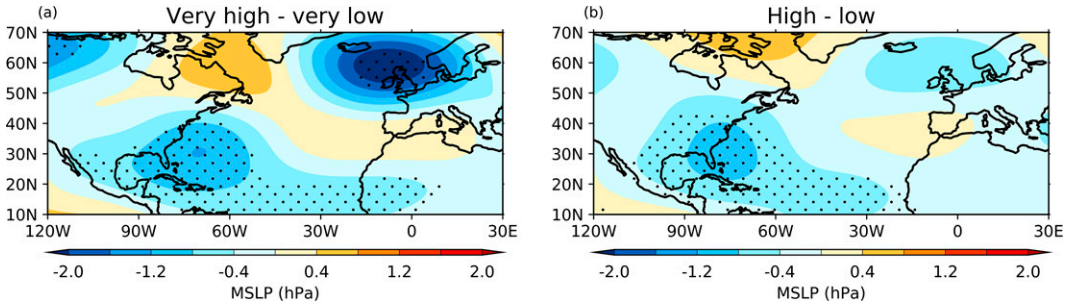

FIG. 6. Composite differences in the ASO mean MSLP field, constructed from 6-hourly T11 spectrally filtered MSLP data. Composites are based on the number of recurving TCs that form in the MDR: (a) very high minus very low (b) high minus low. Stippling denotes significance at 95% using a Student's *t* test.

western subtropical North Atlantic may promote the development of MDR-originating recurving TCs during years of high MDR-originating recurving TC frequency, while the anomalously high MSLP in this region suppresses their development and prohibits their northward migration during years of low MDR-originating recurving TC frequency. However, the significant difference between the composites is not confined to the western subtropical Atlantic and can also be seen in the tropical Atlantic and Caribbean. Negative MSLP anomalies in these regions are associated with decreased atmospheric stability (and therefore increased vertical motion), reduced vertical wind shear, and increased midlevel humidity and temperature, leading to higher TC frequency in the MDR (Klotzbach 2007; Knaff 1997; Saunders et al. 2017). Despite compositing based on recurving TC frequency, the difference between the composites could also arise due to differences in the suitability for TC genesis in the MDR, which leads to differences in recurving TC frequency and indicate a strong association between the TC frequency and recurving TC frequency.

When repeating the analysis in section 3c(1) using MERRA2 spectrally filtered fields (Figs. S1 and S2) instead of ERA5, the results are like those presented here (Figs. 5 and 6), with an anomalous south-easterly flow being present during years that have a high number of recurving TCs. There is a negative difference in MSLP in the western subtropical Atlantic, tropical Atlantic, and Caribbean as is shown in Fig. 6; however, the MERRA2 composites have slightly larger differences, and the largest differences are centered more over the Caribbean for the very high minus very low activity composite.

2) THE STEERING FLOW (SUB)

The analysis shown in section 3c(1) is expanded, this time with composites constructed around the number of recurving TCs that form in the SUB region. Composites are comprised of 6 years that have very high and very low activity, 19 years that have high activity, and 21 years that have low activity. As TCs forming in the SUB region often have much lower LMI (Fig. 4) than those forming in the MDR, they may not extend the entire depth of the troposphere. As a result, the lower tropospheric flow may be a better proxy for their steering flow than the average flow over the entire depth of the troposphere. Figure 7 shows the composite mean difference in the ASO 700-hPa flow for years that have been separated based on SUB recurving TC activity. Anomalous cyclonic flow exists in the subtropical Atlantic during years with many recurving TCs originating in the SUB region. This leads to an anomalous northeasterly flow along the coast of eastern Canada and the Northeast United States. This flow is in the opposite direction to which the recurving TCs forming in the SUB region track (Fig. 3a) and as a result, it does not appear that the anomalous flow pattern would aid TC recurvature. It is

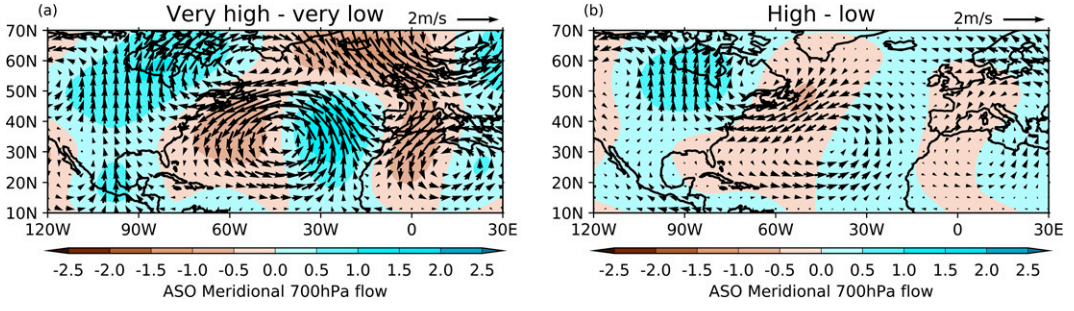

FIG. 7. Composite differences in the ASO mean 700-hPa wind field (wind vectors), constructed from 6-hourly T11 spectrally filtered 700-hPa (u and v) data (all days in ASO). Composites are based on the number of recurving TCs that form in SUB: (a) very high activity minus very low activity and (b) high activity minus low activity. Filled contours show the composite difference in the meridional component of the ASO 700-hPa flow.

therefore unlikely that the seasonal mean steering flow plays a direct role in modulating the recurving TC frequency in the SUB region during the 1979–2018 period. Figure 7 is repeated using the deep layer flow [Eq. (2)], and the flow pattern is the same (Fig. S8).

The anomalous cyclonic circulation that exists in the subtropical North Atlantic during years in which there are a high number of recurving SUB TCs is associated with a reduction in the intensity of the NASH. This may lead to increased TC activity in the SUB region. This contrasts with Fig. 5, wherein the NASH intensity does not differ between years of high and low MDR-originating recurving TC frequency, but where instead the location of the NASH may be more important. The potential relationship between NASH intensity and SUB TC genesis agrees with Kossin et al. (2010), who suggested that a negative NAO (weaker NASH, higher SLP over Iceland) is associated with a higher TC frequency in the subtropical North Atlantic ("cluster 1" therein). Correlation maps between annual SUB TC frequency and the meridional 700-hPa flow show that while correlations do exist in the subtropical North Atlantic between the circulation anomalies and TC activity, these correlations are weak ($r \sim 0.3$) (Fig. S6, supplemental material). Figure 7 is not sensitive to the reanalysis used, with the MERRA2 composite supporting the analysis presented here (Fig. S3).

3) Regional TC activity

In this section, we explore the association between basin-wide TC frequency and recurving TC frequency. To quantify the variability in recurving TC frequency that is associated with TC activity, a multiple linear regression (MLR) model for recurving TC frequency is constructed using two predictors: The number of hurricanes forming in the MDR each year, and the number of TCs (storms of any intensity if present in HURDAT2) forming in the SUB region each year. These predictors are chosen because 85% of recurving TCs originate in either the MDR or SUB regions (Table 1). The majority (81%) of recurving TCs originating in the MDR are of hurricane strength (1-min sustained winds > 33 m s^{-1}) at their LMI (Fig. 4). While Fig. 4 indicates that recurving TCs have a statistically significantly higher LMI in all three regions, the difference between the distributions is considerably larger in the MDR. While stronger TCs are more likely to recurve, MDR major hurricane frequency is not as strongly associated with recurving TC frequency as MDR hurricane frequency (R^2 of 44.2% and 19.7% for MDR hurricane frequency and MDR major hurricane frequency, respectively). This may be because much of the North Atlantic capable of supporting major hurricanes resides in the western side of the basin, where storms have a higher probability of making landfall and subsequently dying out. As a result, the predictors used are MDR hurricane frequency and SUB TC frequency.

Ordinary least squares assumptions are satisfied—there is no collinearity between MDR hurricane number and SUB TC number. The residuals are approximately normally distributed, tested using a Kolmogorov–Smirnov test, and both predictor terms are significant, each explaining a comparable amount of variance of recurving TCs. The variance in the residuals also does not depend on the value of the predicted variable. The fitted MLR model is shown in Eq. (3), where $\mathrm{Rec_{TC}}$, MDR_H, and $\mathrm{SUB_{TC}}$ denote recurving TC frequency, MDR hurricane frequency, and SUB TC frequency, respectively:

$$\mathrm{Rec_{TC}} = 1.053\mathrm{MDR}_H + 0.7539\mathrm{SUB_{TC}} + 0.964 + \epsilon. \quad (3)$$

As this model uses only two predictors, it is unlikely that there is any substantial overfitting. This is tested and confirmed in Figs. 8b and 8c. Using 20 years of data, randomly selected to train the MLR model, the model is then tested on the remaining 20 years of data. This process is iterated 100 000 times to produce the R^2 distribution shown, which has a mean of 75% and a 95% confidence interval of 56%–88%, indicating that there is no substantial overfitting and that the model performs well on the test data. Iterating the process gives us approximately 50 000 predictions for the number of recurving TCs for each year, which are used to construct the 95% confidence interval shown by the shading in Fig. 8.

The resulting MLR model explains 81% of the variance (using all data for the MLR fit) and has an R^2 of 79% when using a leave-one-out cross-validation. Using all data in the regression, the individual R^2 values for the relationship with recurving TC frequency are 33.9% and 42.2% for SUB TC frequency and MDR hurricane frequency, respectively. Figure 8 shows that the interannual variability in the recurving TC number is captured extremely well by the model, indicating that activity in the MDR and SUB regions of the North Atlantic explain most of the variance in the interannual variability of recurving TC frequency.

Poisson regression is often used to investigate the drivers of TC activity (Boudreault et al. 2017; Elsner et al. 2000; Elsner 2003; Elsner et al. 2001; Elsner 1993; Kossin et al. 2010; Kozar et al. 2012; Murakami et al. 2016a) due to the discrete nature of TC counts. To establish robustness, the results presented in Fig. 8 were also reproduced using a Poisson regression model with a logarithmic link function and the results support the analysis presented in this paper (Fig. S12 in the supplemental material).

The sensitivity of the results in Fig. 8 have been tested extensively by changing the domain used to define TC recurvature (Fig. S13), changing the reanalysis used to track the post-tropical stage of the TCs (Fig. S10), and changing the TCs used in the analysis (all TCs in HURDAT versus named storms only, Fig. S11). All of these changes lead to a model that has a fit just as good as presented in Fig. 8.

As TC frequency explains a large fraction of the variance of recurving TC frequency, we investigate the SST anomalies in the North Atlantic during years of high and low MDR hurricane frequency and SUB TC frequency. The SUB TC frequency is not strongly related to tropical Atlantic SSTs and the ENSO state, agreeing with Kossin et al. (2010); however, positive SST anomalies exist along the midlatitude U.S. East Coast during high SUB TC frequency years (Fig. S16). MDR hurricane frequency is highest during La Niña years and years in which there is a positive SST anomaly in the tropical North

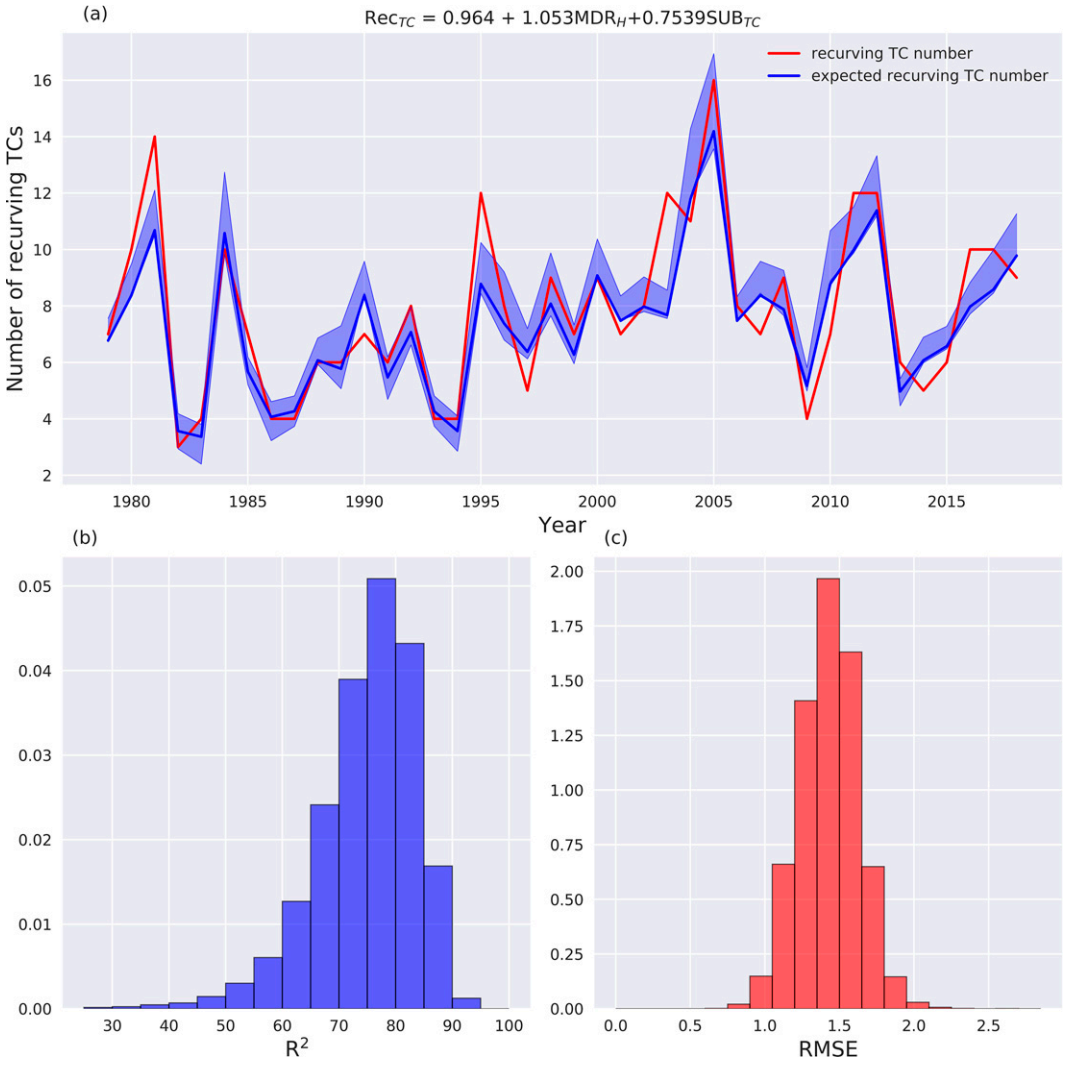

FIG. 8. (a) Recurving TC frequency in the North Atlantic basin between 1979 and 2018 (red) and expected recurving TC frequency in the North Atlantic basin over the same time period, predicted using the multiple linear regression model described in Eq. (3) (blue). Probability distributions of (b) R^2 and (c) RMSE, calculated using a half-and-half test iterated 100 000 times. The shaded region represents the 95% confidence interval, calculated from the half-and-half test.

Atlantic (Fig. S15), which is anticipated based on previous studies (Klotzbach et al. 2017; Landsea et al. 1999; Vecchi et al. 2011).

While the focus of this study is on recurving TCs, it is sensible to ask whether such a strong relationship is seen between TC activity and non-recurving TC frequency. Separating our 40-yr dataset into the 20 years that have a frequency of recurving TCs above and below the mean, we find that the ratio (recurving TCs/non-recurving TCs) is over twice as high for years that have a recurving TC frequency greater than the mean (1.7 and 0.8 for years above and below the mean, respectively). This indicates that years that have a high recurving TC frequency do not necessarily have a high non-recurving TC frequency. However, the correlation between non-recurving TC frequency and basinwide TC frequency is extremely high ($r \sim 0.8$). For recurving TCs, the relationship is with TC activity in the MDR and SUB regions; however, for non-recurving TC frequency, we would anticipate the relationship to be with TC activity in the WEST region, in which most TCs do not recurve (Fig. 1). This would explain why there is a significant relationship between both recurving and non-recurving TC frequency and basinwide TC frequency, but no significant relationship between recurving and non-recurving TC frequency directly.

d. Relative importance of steering flow and TC activity

Figures 5 and 6 indicate that the MSLP and deep layer flow differences exist in the central and western subtropical Atlantic between years associated with high and low recurving TC activity in the MDR, and some of these differences are

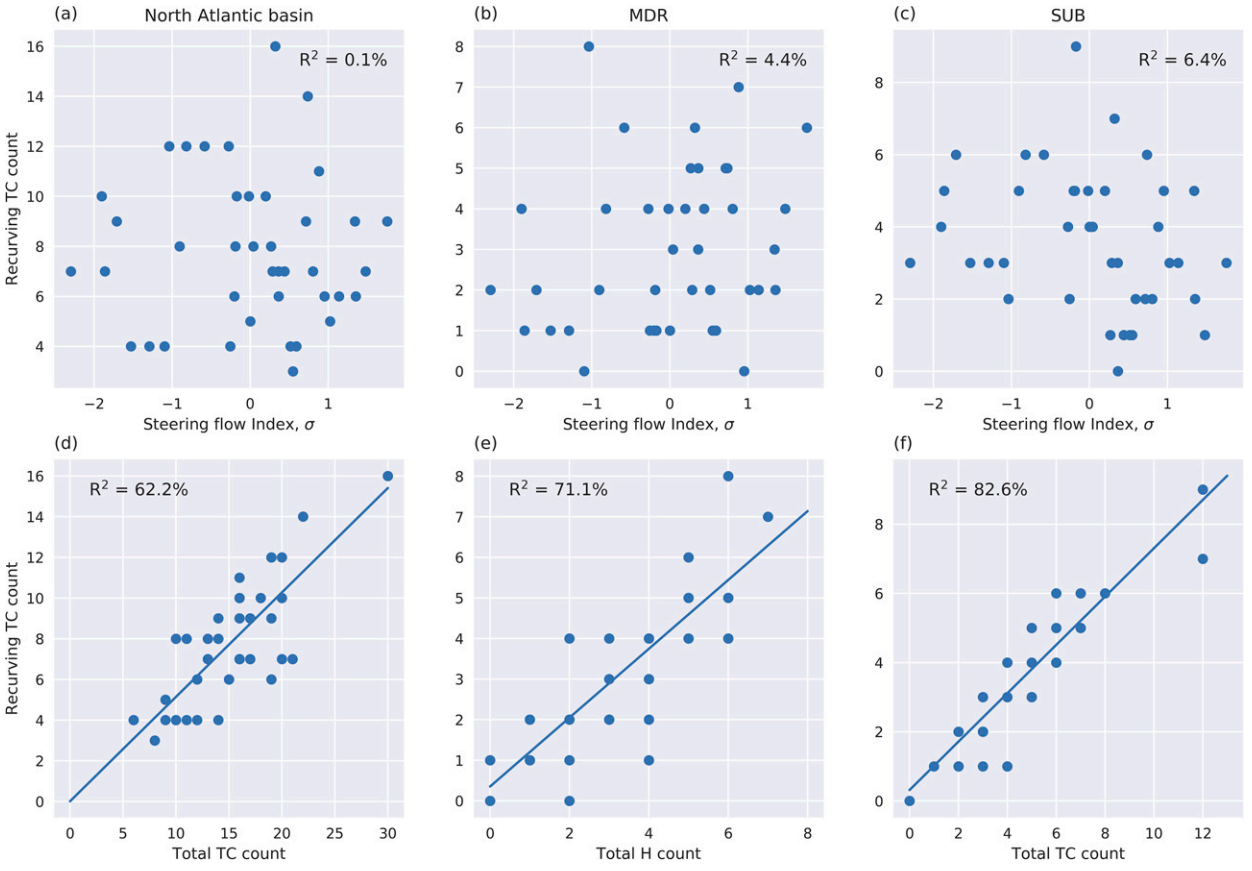

FIG. 9. Annual recurving TC frequency (left) basinwide, (center) originating in the MDR, and (right) originating in the SUB region, against (a)–(c) the steering flow index and (d) basinwide TC activity, (e) hurricanes originating in the MDR, and (f) TCs originating in the SUB region. The meridional component of the deep layer flow in the region 45°–65°W, 25°–35°N is used to create the steering flow index.

physically consistent with our understanding of how the westward extent of the NASH modulates TC recurvature. To quantify the role that the interannual variability of the steering flow plays in modulating recurving TC frequency, we define a steering flow index. This index is created by standardizing the mean ASO meridional component of the deep layer steering flow [Eq. (2)] in a box from 25°–35°N to 45°–65°W. This region was chosen as it captures the largest meridional flow differences in Figs. 5 and 7 and is the region in which the correlation between recurving MDR TC frequency and ASO meridional deep layer steering flow is highest. It is assumed that the meridional (poleward) component of the flow will determine the poleward propagation of TCs rather than the magnitude of the full (u, v) field. We therefore only consider the meridional component of the flow for the index.

Figures 9a–c show the relationship between the number of recurving TCs (basinwide, originating in the MDR, and originating in SUB, respectively) and the steering flow index. Basinwide (Fig. 9a), there is no link between recurving TC frequency and the ASO mean steering flow index. A weak relationship may exist in the MDR and SUB regions (Figs. 9b,c), but correlations between the ASO mean steering flow index and recurving TC frequency are not significant at 95%.

In Fig. 9e, the MDR hurricane frequency is shown instead of MDR TC frequency based on the results of Fig. 4a, which shows that many weak MDR originating TCs die out, and as a result, hurricane number is likely a better predictor. Figure 9 clearly highlights that the interannual variability of recurving TC frequency is modulated by the frequency with which hurricanes form in the MDR and TCs form in SUB (Figs. 9e,f), with interannual variability in the seasonal mean steering flow potentially playing a small, secondary role. A second-order effect may also come from interannual variability in genesis location, particularly within the SUB region. The result remains unchanged when Fig. 9 is reproduced using MERRA2 data (Fig. S4), indicating that it is not sensitive to the reanalysis used.

The TC activity and the seasonal mean steering flow are not completely independent. The NAO index, which in part depends on the strength and location of the NASH is (weakly) associated with TC frequency in the subtropical Atlantic. A weaker NASH may also reduce the pressure gradient between the subtropical Atlantic and the equator, reducing trade wind strength, leading to higher SSTs and enhanced TC frequency. Correlation maps (Fig. S14) have shown that these correlations are weak ($r \sim 0.2$–0.3) and not

significant, so collinearity between steering and TC activity in the MLR model is unlikely. Interannually, the steering flow is not strongly or significantly associated with basinwide TC frequency, but TC frequency is strongly and significantly associated with recurving TC frequency.

4. Discussion and conclusions

The aim of this paper is to investigate the relative importance of the interannual variability of TC frequency and the steering flow in governing North Atlantic recurving TC frequency. This is achieved using a track matching algorithm to identify observed TC tracks from HURDAT2 in the ERA5 and MERRA2 reanalyses. This provides extended information about the precursor and post-tropical stages of storms beyond what is available in HURDAT2 alone, which is then used to objectively identify the recurving TCs. We then partition the storms into three subregions based on genesis location [main development region (MDR), subtropical North Atlantic (SUB), and the region comprising of the Gulf of Mexico and south Caribbean (WEST)]. The main conclusions of this study are as follows:

- Over 75% of the variance in seasonal North Atlantic recurving TC frequency can be explained by just two predictors: seasonal TC frequency originating in the subtropical Atlantic region, and seasonal hurricane (1-min sustained winds > 33 m s^{-1}) frequency originating in the main development region. The individual R^2 (using all data) are 33.9% for subtropical Atlantic TC frequency and 42.2% for main development region hurricane frequency.
- Only a weak relationship between the meridional component of the seasonal mean deep layer steering flow and recurving TC frequency is found, which is not significant.
- TC frequency explains most of the variability in recurving TC frequency, with interannual variability in the steering flow and genesis latitude potentially playing smaller, secondary roles.

The methods used here are robust to the different reanalyses used to track the TCs, to the boundaries of the domain used to define recurvature, and to the cyclones in HURDAT2 used (all TCs or just those with winds > 17 m s^{-1}).

We are not suggesting that the steering flow is unimportant for TC recurvature–on the time scales of individual TCs, the steering flow is crucial for their steering and evolution. But on the seasonal time scale, the interannual variability in TC frequency is much more strongly associated with the interannual variability of recurving TC frequency than the interannual variability in the steering flow. This result suggests that skillful seasonal forecasts of Atlantic hurricane activity could also increase seasonal forecast skill in regions primarily impacted by recurving TCs, such as the east coasts of the U.S. and Canada, and Europe.

The results presented here may also help us to understand how recurving TC frequency might change in the future. A small decrease is expected in TC counts in the North Atlantic due to climate change; particularly a decrease in weaker, short-lived TCs (Knutson et al. 2019). However, the TCs that do form will likely be more intense at their LMI than in the current climate (Knutson et al. 2019). There already appears to be a poleward migration in the latitude at which TCs attain their LMI (Kossin et al. 2014) and if anthropogenically driven, this will likely persist into the future. Given the poleward shift in LMI and expected increase in the average intensity of TCs (suggesting increased longevity), coupled with the knowledge that weak, short-lived TCs (particularly those forming in the MDR) are unlikely to recurve, the North Atlantic may see more recurving TCs in the future, proportionally and possibly also in terms of absolute counts. Climate model projections should be utilized to further understand how recurving TC frequency and their direct and downstream impacts may change in the future, using high-resolution climate models in particular (such as in Haarsma et al. 2013; Roberts et al. 2020) that better capture the intensity of TCs.

Acknowledgments. E. Sainsbury was funded by the Natural Environment Research Council (NERC) via the SCENARIO Doctoral Training Partnership (Grant NE/S0077261/1) with additional CASE funding from BP. R.S., K. H., A. B., and L.S. are supported by the U.K. National Centre for Atmospheric Science (NCAS) at the University of Reading. A.B. also acknowledges PRIMAVERA funding received from the European Commission under Grant 641727 of the Horizon 2020 research program and funding from NERC through The North Atlantic Climate System Integrated Study (ACSIS) Grant NE/N018044/1. We thank Baoqiang Xiang and two anonymous reviewers for their comments, which greatly improved the quality and clarity of the manuscript.

Data availability statement. HURDAT2 data can be downloaded at aoml.noaa.gov/hrd/hurdat/. Reanalysis data used for cyclone tracking and composite analysis can be obtained from https://disc.gsfc.nasa.gov/ (MERRA2) and from the Copernicus C3S Date store (https://www.ecmwf.int/en/forecasts/datasets/reanalysis-datasets/era5) for ERA5. Both reanalyses are freely available. TRACK is available for use with permission (see https://gitlab.act.reading.ac.uk/track/track, version 1.5.2 used).

REFERENCES

Aiyyer, A. R., and C. Thorncroft, 2006: Climatology of vertical wind shear over the tropical Atlantic. *J. Climate*, **19**, 2969–2983, https://doi.org/10.1175/JCLI3685.1.

Archambault, H. M., L. F. Bosart, D. Keyser, and J. M. Cordeira, 2013: A climatological analysis of the extratropical flow response to recurving western North Pacific tropical cyclones. *Mon. Wea. Rev.*, **141**, 2325–2346, https://doi.org/10.1175/MWR-D-12-00257.1.

Arnault, J., and F. Roux, 2011: Characteristics of African easterly waves associated with tropical cyclogenesis in the Cape Verde Islands region in July-August-September of 2004–2008. *Atmos. Res.*, **100**, 61–82, https://doi.org/10.1016/j.atmosres.2010.12.028.

Baker, A. J., K. I. Hodges, R. K. H. Schiemann, and P. L. Vidale, 2021: Historical variability and lifecycles of North Atlantic midlatitude cyclones originating in the tropics. *J. Geophys.*

Res. Atmos., **126**, e2020JD033924, https://doi.org/10.1029/2020JD033924.

Bell, B., and Coauthors, 2021: The ERA5 global reanalysis: Preliminary extension to 1950. *Quart. J. Roy. Meteor. Soc.*, **147**, 4186–4227, https://doi.org/10.1002/qj.4174.

Bhatia, K., A. Baker, G. Vecchi, H. Murakami, J. Kossin, P. Luigi, K. Hodges, and T. Knutson, 2020: An environmental explanation for the recent increase in tropical cyclone intensification. *EGU General Assembly 2020*, online, EGU, EGU2020-18644, https://doi.org/10.5194/egusphere-egu2020-18644.

Blake, E. S., T. B. Kimberlain, R. J. Berg, J. P. Cangialosi, and J. L. Beven II, 2013: Tropical cyclone report: Hurricane Sandy (22–29 October 2012). National Hurricane Center Tropical Cyclone Rep. AL182012, 157 pp., https://www.nhc.noaa.gov/data/tcr/AL182012_Sandy.pdf.

Boudreault, M., L. P. Caron, and S. J. Camargo, 2017: Reanalysis of climate influences on Atlantic tropical cyclone activity using cluster analysis. *J. Geophys. Res. Atmos.*, **122**, 4258–4280, https://doi.org/10.1002/2016JD026103.

Camargo, S. J., M. Ting, and Y. Kushnir, 2013: Influence of local and remote SST on North Atlantic tropical cyclone potential intensity. *Climate Dyn.*, **40**, 1515–1529, https://doi.org/10.1007/s00382-012-1536-4.

Camp, J., M. Roberts, C. Maclachlan, E. Wallace, L. Hermanson, A. Brookshaw, A. Arribas, and A. A. Scaife, 2015: Seasonal forecasting of tropical storms using the Met Office GloSea5 seasonal forecast system. *Quart. J. Roy. Meteor. Soc.*, **141**, 2206–2219, https://doi.org/10.1002/qj.2516.

Caron, L. P., and C. G. Jones, 2012: Understanding and simulating the link between African easterly waves and Atlantic tropical cyclones using a regional climate model: The role of domain size and lateral boundary conditions. *Climate Dyn.*, **39**, 113–135, https://doi.org/10.1007/s00382-011-1160-8.

Chan, J. C. L., and W. M. Gray, 1982: Tropical cyclone movement and surrounding flow relationships. *Mon. Wea. Rev.*, **110**, 1354–1374, https://doi.org/10.1175/1520-0493(1982)110<1354:TCMASF>2.0.CO;2.

Colbert, A. J., and B. J. Soden, 2012: Climatological variations in North Atlantic tropical cyclone tracks. *J. Climate*, **25**, 657–673, https://doi.org/10.1175/JCLI-D-11-00034.1.

Dekker, M. M., R. J. Haarsma, H. de Vries, M. Baatsen, and A. J. van Delden, 2018: Characteristics and development of European cyclones with tropical origin in reanalysis data. *Climate Dyn.*, **50**, 445–455, https://doi.org/10.1007/s00382-017-3619-8.

Delgado, S., C. W. Landsea, and H. Willoughby, 2018: Reanalysis of the 1954–63 Atlantic hurricane seasons. *J. Climate*, **31**, 4177–4192, https://doi.org/10.1175/JCLI-D-15-0537.1.

Elsner, J. B., 2003: Tracking hurricanes. *Bull. Amer. Meteor. Soc.*, **84**, 353–356, https://doi.org/10.1175/BAMS-84-3-353.

——, and C. P. Schmertmann, 1993: Improving extended-range seasonal predictions of intense Atlantic hurricane activity. *Wea. Forecasting*, **8**, 345–351, https://doi.org/10.1175/1520-0434(1993)008<0345:IERSPO>2.0.CO;2.

——, K. Liu, and B. Kocher, 2000: Spatial variations in major U.S. hurricane activity: Statistics and a physical mechanism. *J. Climate*, **13**, 2293–2305, https://doi.org/10.1175/1520-0442(2000)013<2293:SVIMUS>2.0.CO;2.

——, B. H. Bossak, and X. F. Niu, 2001: Secular changes to the ENSO-U.S. hurricane relationship. *Geophys. Res. Lett.*, **28**, 4123–4126, https://doi.org/10.1029/2001GL013669.

Evans, C., and Coauthors, 2017: The extratropical transition of tropical cyclones. Part I: Cyclone evolution and direct impacts. *Mon. Wea. Rev.*, **145**, 4317–4344, https://doi.org/10.1175/MWR-D-17-0027.1.

Gelaro, R., and Coauthors, 2017: The Modern-Era Retrospective Analysis for Research and Applications, version 2 (MERRA-2). *J. Climate*, **30**, 5419–5454, https://doi.org/10.1175/JCLI-D-16-0758.1.

Haarsma, R. J., W. Hazeleger, C. Severijns, H. De Vries, A. Sterl, R. Bintanja, G. J. Van Oldenborgh, and H. W. Van Den Brink, 2013: More hurricanes to hit western Europe due to global warming. *Geophys. Res. Lett.*, **40**, 1783–1788, https://doi.org/10.1002/grl.50360.

Hagen, A. B., D. Strahan-Sakoskie, and C. Luckett, 2012: A reanalysis of the 1944–53 Atlantic hurricane seasons-the first decade of aircraft reconnaissance. *J. Climate*, **25**, 4441–4460, https://doi.org/10.1175/JCLI-D-11-00419.1.

Harr, P. A., and R. L. Elsberry, 1995: Large-scale circulation variability over the tropical western North Pacific. Part I: Spatial patterns and tropical cyclone characteristics. *Mon. Wea. Rev.*, **123**, 1225–1246, https://doi.org/10.1175/1520-0493(1995)123<1225:LSCVOT>2.0.CO;2.

Hersbach, H., and Coauthors, 2020: The ERA5 global reanalysis. *Quart. J. Roy. Meteor. Soc.*, **146**, 1999–2049, https://doi.org/10.1002/qj.3803.

Hickney, K. R., and C. Connolly-Johnston, 2012: The impact of Hurricane Debbie (1961) and Hurricane Charley (1986) on Ireland. *Advances in Hurricane Research: Modelling, Meteorology, Preparedness and Impacts*, 1st ed. K. R. Hickey, Ed., INTECH, 183–198.

Hodges, K. I., 1994: A general method for tracking analysis and its application to meteorological data. *Mon. Wea. Rev.*, **122**, 2573–2586, https://doi.org/10.1175/1520-0493(1994)122<2573:AGMFTA>2.0.CO;2.

——, 1995: Feature tracking on the unit sphere. *Mon. Wea. Rev.*, **123**, 3458–3465, https://doi.org/10.1175/1520-0493(1995)123<3458:FTOTUS>2.0.CO;2.

——, 1996: Spherical nonparametric estimators applied to the UGAMP model integration for AMIP. *Mon. Wea. Rev.*, **124**, 2914–2932, https://doi.org/10.1175/1520-0493(1996)124<2914:SNEATT>2.0.CO;2.

——, 1999: Adaptive constraints for feature tracking. *Mon. Wea. Rev.*, **127**, 1362–1373, https://doi.org/10.1175/1520-0493(1999)127<1362:ACFFT>2.0.CO;2.

——, 2008: Confidence intervals and significance tests for spherical data derived from feature tracking. *Mon. Wea. Rev.*, **136**, 1758–1777, https://doi.org/10.1175/2007MWR2299.1.

——, and R. Emerton, 2015: The prediction of Northern Hemisphere tropical cyclone extended life cycles by the ECMWF ensemble and deterministic prediction systems. Part I: Tropical cyclone stage. *Mon. Wea. Rev.*, **143**, 5091–5114, https://doi.org/10.1175/MWR-D-13-00385.1.

——, A. Cobb, and P. L. Vidale, 2017: How well are tropical cyclones represented in reanalysis datasets? *J. Climate*, **30**, 5243–5264, https://doi.org/10.1175/JCLI-D-16-0557.1.

Jones, S. C., and Coauthors, 2003: The extratropical transition of tropical cyclones: Forecast challenges, current understanding, and future directions. *Wea. Forecasting*, **18**, 1052–1092, https://doi.org/10.1175/1520-0434(2003)018<1052:TETOTC>2.0.CO;2.

Kelly, P., L. R. Leung, K. Balaguru, W. Xu, B. Mapes, and B. Soden, 2018: Shape of Atlantic tropical cyclone tracks and the Indian monsoon. *Geophys. Res. Lett.*, **45**, 10 746–10 755, https://doi.org/10.1029/2018GL080098.

Klotzbach, P. J., 2007: Revised prediction of seasonal Atlantic basin tropical cyclone activity from 1 August. *Wea. Forecasting*, **22**, 937–949, https://doi.org/10.1175/WAF1045.1.

——, 2014: Prediction of seasonal Atlantic basin accumulated cyclone energy from 1 July. *Wea. Forecasting*, **29**, 115–121, https://doi.org/10.1175/WAF-D-13-00073.1.

——, M. A. Saunders, G. D. Bell, and E. S. Blake, 2017: North Atlantic seasonal hurricane prediction: Underlying science and an evaluation of statistical models. *Climate Extremes*, **226**, 315–328, https://doi.org/10.1002/9781119068020.ch19.

——, and Coauthors, 2019: Seasonal tropical cyclone forecasting. *Trop. Cyclone Res. Rev.*, **8**, 134–149, https://doi.org/10.1016/j.tcrr.2019.10.003.

Knaff, J. A., 1997: Implications of summertime sea level pressure anomalies in the tropical Atlantic region. *J. Climate*, **10**, 789–804, https://doi.org/10.1175/1520-0442(1997)010<0789:IOSSLP>2.0.CO;2.

Knutson, T., and Coauthors, 2019: Tropical cyclones and climate change assessment. Part I: Detection and attribution. *Bull. Amer. Meteor. Soc.*, **100**, 1987–2007, https://doi.org/10.1175/BAMS-D-18-0189.1.

Kossin, J. P., S. J. Camargo, and M. Sitkowski, 2010: Climate modulation of North Atlantic hurricane tracks. *J. Climate*, **23**, 3057–3076, https://doi.org/10.1175/2010JCLI3497.1.

——, K. A. Emanuel, and G. A. Vecchi, 2014: The poleward migration of the location of tropical cyclone maximum intensity. *Nature*, **509**, 349–352, https://doi.org/10.1038/nature13278.

Kozar, M. E., M. E. Mann, S. J. Camargo, J. P. Kossin, and J. L. Evans, 2012: Stratified statistical models of North Atlantic basin-wide and regional tropical cyclone counts. *J. Geophys. Res.*, **117**, D18103, https://doi.org/10.1029/2011JD017170.

Landsea, C. W., and J. L. Franklin, 2013: Atlantic hurricane database uncertainty and presentation of a new database format. *Mon. Wea. Rev.*, **141**, 3576–3592, https://doi.org/10.1175/MWR-D-12-00254.1.

——, R. A. Pielke Jr., A. M. Mestas-Nunez, and J. A. Knaff, 1999: Atlantic basin hurricanes: Indices of climate changes. *Climatic Change*, **42**, 89–129, https://doi.org/10.1023/A:1005416332322.

Laurila, T. K., V. A. Sinclair, and H. Gregow, 2020: The extratropical transition of Hurricane Debby (1982) and the subsequent development of an intense windstorm over Finland. *Mon. Wea. Rev.*, **148**, 377–401, https://doi.org/10.1175/MWR-D-19-0035.1.

Molod, A., L. Takacs, M. Suarez, and J. Bacmeister, 2015: Development of the GEOS-5 atmospheric general circulation model: Evolution from MERRA to MERRA2. *Geosci. Model Dev.*, **8**, 1339–1356, https://doi.org/10.5194/gmd-8-1339-2015.

Murakami, H., and Coauthors, 2016a: Seasonal forecasts of major hurricanes and landfalling tropical cyclones using a high-resolution GFDL coupled climate model. *J. Climate*, **29**, 7977–7989, https://doi.org/10.1175/JCLI-D-16-0233.1.

——, G. Villarini, G. A. Vecchi, W. Zhang, and R. Gudgel, 2016b: Statistical-dynamical seasonal forecast of North Atlantic and U.S. landfalling tropical cyclones using the high-resolution GFDL FLOR coupled model. *Mon. Wea. Rev.*, **144**, 2101–2123, https://doi.org/10.1175/MWR-D-15-0308.1.

Rappaport, E. N., and Coauthors, 2009: Advances and challenges at the National Hurricane Center. *Wea. Forecasting*, **24**, 395–419, https://doi.org/10.1175/2008WAF2222128.1.

Riboldi, J., M. Röthlisberger, and C. M. Grams, 2018: Rossby wave initiation by recurving tropical cyclones in the western North Pacific. *Mon. Wea. Rev.*, **146**, 1283–1301, https://doi.org/10.1175/MWR-D-17-0219.1.

Roberts, M. J., and Coauthors, 2020: Projected future changes in tropical cyclones using the CMIP6 HighResMIP multimodel ensemble. *Geophys. Res. Lett.*, **47**, e2020GL088662, https://doi.org/10.1029/2020GL088662.

Sainsbury, E. M., R. K. H. Schiemann, K. I. Hodges, L. C. Shaffrey, A. J. Baker, and K. T. Bhatia, 2020: How important are post-tropical cyclones for European windstorm risk? *Geophys. Res. Lett.*, **47**, e2020GL089853, https://doi.org/10.1029/2020GL089853.

Saunders, M. A., P. J. Klotzbach, and A. S. R. Lea, 2017: Replicating annual North Atlantic hurricane activity 1878–2012 from environmental variables. *J. Geophys. Res. Atmos.*, **122**, 6284–6297, https://doi.org/10.1002/2017JD026492.

Varlas, G., A. Papadopoulos, and P. Katsafados, 2019: An analysis of the synoptic and dynamical characteristics of Hurricane Sandy (2012). *Meteor. Atmos. Phys.*, **131**, 443–453, https://doi.org/10.1007/s00703-017-0577-y.

Vecchi, G. A., M. Zhao, H. Wang, G. Villarini, A. Rosati, A. Kumar, I. M. Held, and R. Gudgel, 2011: Statistical-dynamical predictions of seasonal North Atlantic hurricane activity. *Mon. Wea. Rev.*, **139**, 1070–1082, https://doi.org/10.1175/2010MWR3499.1.

Wang, B., X. Li, and L. Wu, 1997: Direction of hurricane beta drift in horizontally sheared flows. *J. Atmos. Sci.*, **54**, 1462–1471, https://doi.org/10.1175/1520-0469(1997)054<1462:DOHBDI>2.0.CO;2.

——, Y. Wang, and L. Wu, 1998: Dynamics in tropical cyclone motion: A review. *Chin. J. Atmos. Sci.*, **22**, 416–434.